



LAWRENCE
LIVERMORE
NATIONAL
LABORATORY

Toward TeV Conformality

T. Appelquist, A. Avakian, R. Babich, R. C. Brower, M. Cheng, M. A. Clark, S. D. Cohen, G. T. Fleming, J. Kiskis, E. T. Neil, J. C. Osborn, C. Rebbi, D. Schaich, R. Soltz, P. Vranas

December 1, 2009

Physical Review Letters

Disclaimer

This document was prepared as an account of work sponsored by an agency of the United States government. Neither the United States government nor Lawrence Livermore National Security, LLC, nor any of their employees makes any warranty, expressed or implied, or assumes any legal liability or responsibility for the accuracy, completeness, or usefulness of any information, apparatus, product, or process disclosed, or represents that its use would not infringe privately owned rights. Reference herein to any specific commercial product, process, or service by trade name, trademark, manufacturer, or otherwise does not necessarily constitute or imply its endorsement, recommendation, or favoring by the United States government or Lawrence Livermore National Security, LLC. The views and opinions of authors expressed herein do not necessarily state or reflect those of the United States government or Lawrence Livermore National Security, LLC, and shall not be used for advertising or product endorsement purposes.

Toward TeV Conformality

T. Appelquist,¹ A. Avakian,² R. Babich,² R. C. Brower,² M. Cheng,³ M. A. Clark,^{4,5} S. D. Cohen,² G. T. Fleming,¹ J. Kiskis,⁶ E. T. Neil,¹ J. C. Osborn,⁷ C. Rebbi,² D. Schaich,² R. Soltz,³ and P. Vranas³

(Lattice Strong Dynamics (LSD) Collaboration)

¹*Department of Physics, Sloane Laboratory, Yale University, New Haven, CT 06520*

²*Department of Physics, Boston University, Boston, MA 02215*

³*Physical Sciences Directorate, Lawrence Livermore National Laboratory, Livermore, CA 94550*

⁴*Harvard-Smithsonian Center for Astrophysics, Cambridge, MA 02138*

⁵*Initiative in Innovative Computing, Harvard University School of Engineering and Applied Sciences, Cambridge, MA 02138*

⁶*Department of Physics, University of California, Davis, CA 95616*

⁷*Argonne Leadership Computing Facility, Argonne, IL 60439*

We study the chiral condensate $\langle\bar{\psi}\psi\rangle$ for an $SU(3)$ gauge theory with N_f massless Dirac fermions in the fundamental representation when N_f is increased from 2 to 6. For $N_f = 2$, our lattice simulations of $\langle\bar{\psi}\psi\rangle/F^3$, where F is the Nambu-Goldstone-boson decay constant, agree with the measured QCD value. For $N_f = 6$, this ratio shows significant enhancement, presaging an even larger enhancement anticipated as N_f increases further, toward the critical value for transition from confinement to infrared conformality.

PACS numbers: 11.10.Hi, 11.15.Ha, 11.25.Hf, 12.60.Nz, 11.30.Qc

Introduction Theories with an approximate conformal symmetry could play a role in describing new physics at the TeV scale and beyond. While a non-supersymmetric, vector-like gauge theory exhibits confinement and spontaneous chiral symmetry breaking with a small number N_f of massless fermions, it becomes conformal in the infrared, governed by a weak infrared fixed point if N_f is larger, but just below the value for which asymptotic freedom sets in [1]. There is evidence from lattice simulations [2, 3, 4, 5, 6] that this infrared conformality persists down through a “conformal window” of N_f -values where the fixed point can become strong, and that a transition to the confining and chirally broken phase takes place at some value N_f^c .

Even for $N_f < N_f^c$ there can remain an approximate infrared fixed point providing that $0 < N_f^c - N_f \ll N_f^c$. The scale F of chiral symmetry breaking is then small relative to the intrinsic scales of the theory, and the fixed point approximately governs the theory from the breaking scale out to some higher scale.

This “walking” phenomenon can play an important phenomenological role in a technicolor theory of electroweak symmetry breaking. (If there are $N_f/2$ electroweak doublets, then $F = F_{EW}/\sqrt{N_f/2} \simeq 250 \text{ GeV}/\sqrt{N_f/2}$.) Flavor-changing neutral currents (FCNC’s), which are present when the technicolor theory is extended to provide for the generation of quark masses, can be too large unless the associated scale Λ_{ETC} is high enough. But then the first- and second-generation quark masses are typically much too small. They are proportional to the quantity $\langle\bar{\psi}\psi\rangle/\Lambda_{ETC}^2$, where ψ is a technifermion field and $\langle\bar{\psi}\psi\rangle$ is the bilinear fermion condensate defined (cut off) at Λ_{ETC} . Walking can lift the quark masses by enhancing the condensate $\langle\bar{\psi}\psi\rangle$ significantly above its value ($O(4\pi F^3)$) in a QCD-like theory, while keeping Λ_{ETC}^2 large enough to

suppress FCNC’s.

The enhancement of $\langle\bar{\psi}\psi\rangle/F^3$ as $N_f \rightarrow N_f^c$ from below has been indicated by Feynman-graph-based studies [7, 8]. But it is important also to use non-perturbative methods since the couplings involved are strong. This letter describes a first step in this program. We focus on an $SU(3)$ gauge theory with N_f massless Dirac fermions in the fundamental representation. Lattice studies have shown that the $N_f = 8$ theory is chirally broken, with no evidence for even an approximate infrared fixed point [2, 4]; while there is significant lattice evidence for conformal behavior at $N_f = 12$, indicating that $8 < N_f^c < 12$ [2, 3, 4, 5, 6].

We present results here for the values $N_f = 2$ and $N_f = 6$, drawing on newly available computational resources, including 150 million core-hours on the Blue-Genie/L supercomputer at Lawrence Livermore National Laboratory (LLNL). Starting with $N_f = 2$ allows us to check the reliability of our methods by comparison with the phenomenological value of $\langle\bar{\psi}\psi\rangle/F^3$ for QCD. Proceeding carefully toward N_f^c is prudent since the emergence of widely separated scales associated with the approximate infrared fixed point of walking is problematic for lattice methods. Still, inspection of our lattice results at $N_f = 6$ indicates an enhancement of $\langle\bar{\psi}\psi\rangle/F^3$ of at least 50%, and even a very conservative lower bound based on chiral perturbation theory (χ PT) indicates significant enhancement.

Methods For a range of small fermion masses m , we compute the Nambu-Goldstone-boson (NGB) mass M_m , the NGB decay constant F_m , and the chiral condensate per fermion $\langle\bar{\psi}\psi\rangle_m$. To set a physical scale, we also compute the mass $M_{\rho,m}$ of the analogue of the ρ meson and the Sommer scale $r_{0,m}$ at which $r^2 dV(r)/dr = 1.65$, where $V(r)$ is the static potential [9]. Since our goal is to search for the enhancement of $\langle\bar{\psi}\psi\rangle/F^3$ as $N_f \rightarrow N_f^c$, from the emergence of walking between the physical length

scale and the ultraviolet cutoff, taken here to be the lattice spacing, it is important to keep the lattice spacing fixed (and small) in physical units. We first choose a value for $\beta \equiv 6/g_0^2$ at $N_f = 6$, giving a physical scale of several lattice units. For $N_f = 2$, we then tune β to match the same physical scale in lattice units. The resultant enhancement is lattice-sensitive, but we expect it to match qualitatively the enhancement with a physical, continuum cutoff.

If the fermion masses are small enough, then the extrapolation $m \rightarrow 0$ can be carried out by fitting the results for M_m^2 , F_m and $\langle \bar{\psi}\psi \rangle_m$ to χ PT. The next-to-leading-order (NLO) expressions are [10]

$$M_m^2 = \frac{2m\langle \bar{\psi}\psi \rangle}{F^2} \left\{ 1 + zm \left[\alpha_M + \frac{1}{N_f} \log(zm) \right] \right\}, \quad (1)$$

$$F_m = F \left\{ 1 + zm \left[\alpha_F - \frac{N_f}{2} \log(zm) \right] \right\}, \quad (2)$$

$$\langle \bar{\psi}\psi \rangle_m = \langle \bar{\psi}\psi \rangle \left\{ 1 + zm \left[\alpha_C - \frac{N_f^2 - 1}{N_f} \log(zm) \right] \right\}, \quad (3)$$

where $z = 2\langle \bar{\psi}\psi \rangle / (4\pi)^2 F^4$.

There is a contribution to $\langle \bar{\psi}\psi \rangle_m$ linear in m and quadratically sensitive to the UV cutoff, present even without spontaneous chiral symmetry breaking. This “contact term”, incorporated here (with a slight abuse of notation) into α_C , is independent of N_f . It dominates α_C , and in fact dominates $\langle \bar{\psi}\psi \rangle_m$ for the entire range of m values in our simulations. The chiral-log terms in F_m and $\langle \bar{\psi}\psi \rangle_m$ grow essentially linearly with N_f , while the chiral-log term in M_m^2 falls. Each of the (unknown) coefficients α_M , α_F and α_C of the analytic terms has a piece, not shown explicitly, that grows linearly with N_f .

For small enough m , the benchmark mass $M_{\rho,m}$ can also be extrapolated $m \rightarrow 0$ using a fit derived from χ PT [11]. Here the NLO term is linear in m (there is no $m \log(m)$ term). Similarly, the NLO term in the chiral expansion of $r_{0,m}$ is linear in m .

Simulation Details We use domain wall fermions with the Iwasaki improved gauge action, as used by the RBC-UKQCD collaboration [12]. Lattice fermion discretization typically breaks chiral symmetry, but in the domain wall formulation the breaking is exponentially suppressed (with flavor symmetry preserved), making it ideal for the study of chiral dynamics. Gauge configurations are generated using the hybrid Monte Carlo method as implemented in the USQCD application libraries, in particular CPS, via a multi-level symplectic integrator, and using Hasenbusch preconditioning and chronological inversion. Autocorrelation is reduced by blocking over sets of 50 trajectories.

The lattice volume is set to $32^3 \times 64$, with the length of the fifth dimension $L_s = 16$ and the domain-wall height $m_0 = 1.8$. All quantities are given in lattice units. For $N_f = 6$ we choose $\beta = 2.10$. For $N_f = 2$ the choice

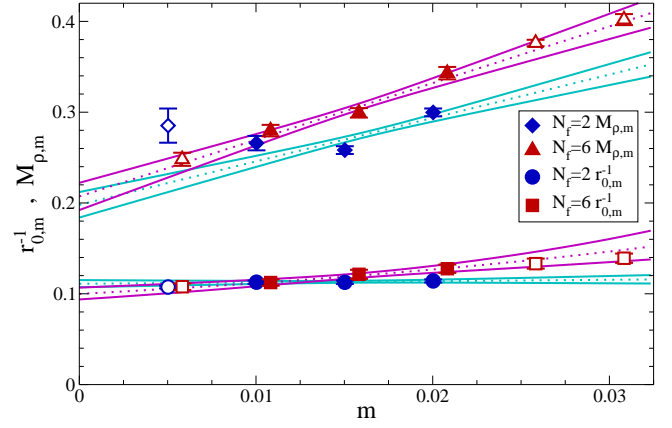


FIG. 1: Linear chiral extrapolations of $M_{\rho,m}$ and the Sommer scale $r_{0,m}^{-1}$, in lattice units, based on the (solid) points at $m_f = 0.01 - 0.02$. Both show agreement within error between $N_f = 2$ and $N_f = 6$ in the chiral limit.

$\beta = 2.70$ then leads to nearly the same physical scale in lattice units. Simulations are performed for fermion masses $m_f = 0.005$ to 0.03 . At finite lattice spacing, even with $m_f = 0$, the chiral symmetry is not exact, with the violation captured in a residual mass $m_{res} \ll m_f$. The total fermion mass m is then $m \equiv m_f + m_{res}$.

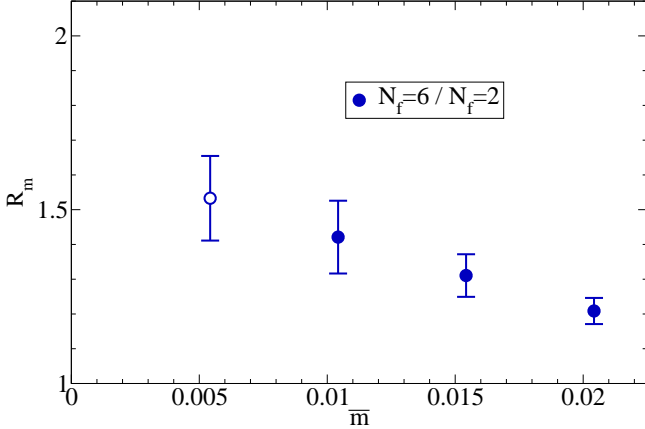
Although global topological charge, Q , is an irrelevant quantity with massless fermions and infinite volume, in a finite volume it becomes relevant [13]. On a discretized lattice, Q is not conserved, with the system evolving between sectors, an evolution crucial for the correct sampling of the path integral at finite volume. With very light fermions, the evolution of Q slows dramatically using current Monte Carlo methods [14]. We find that Q evolves sufficiently for $m_f \geq 0.01$ for both $N_f = 2$ and 6 . At $m_f = 0.005$ it does not, leading to systematic shifts in $\langle \bar{\psi}\psi \rangle_m$ and F_m , which we will explore in a future paper. Here, we present results for $m_f = 0.005$, but do not include them in our analysis. This also ensures that for each m , $M_m L > 4$, keeping the NGB Compton wavelength well inside the lattice. For $N_f = 6$, there are also results for $m_f = 0.025, 0.03$, but they are not used in any chiral extrapolations.

Results Values for $M_{\rho,m}$ and $1/r_{0,m}$ are shown in Fig. 1. The small change in these quantities in the range $m = 0.01 - 0.02$, and the absence of $m \log(m)$ terms in the small- m expansion suggests that the leading, linear terms should dominate here even for $N_f = 6$. Thus we extrapolate $m \rightarrow 0$ using linear fits. The extrapolated values of M_ρ and $1/r_{0,m}$ for $N_f = 2$ are the same within errors as the $N_f = 6$ values, indicating that the physical scale is well matched in lattice units. Numerical values are given in Table I. For QCD, $r_0 = 0.378(9) \text{ GeV}^{-1}$ [15], giving $1/M_\rho r_0 = 0.488(12)$, in reasonable agreement with our $N_f = 2$ value $1/M_\rho r_0 = 0.561(44)$.

Turning now to M_m^2 , F_m , and $\langle \bar{\psi}\psi \rangle_m$, and noting that $M_m^2/2mF_m$ extrapolates to $\langle \bar{\psi}\psi \rangle/F^3$ in the chiral limit,

N_f	$1/r_0$	M_ρ	$\langle\bar{\psi}\psi\rangle/F^2$	F	$\langle\bar{\psi}\psi\rangle$
2	0.111(4)	0.198(14)	0.99(17)	0.0209(41)	$4.32(94) \times 10^{-4}$
6	0.100(6)	0.207(15)	—	—	—
N_f	z	α_M	α_F	α_C	$\chi^2/\text{d.o.f.}$
2	28(16)	0.31(62)	0.64(47)	83(29)	6.50

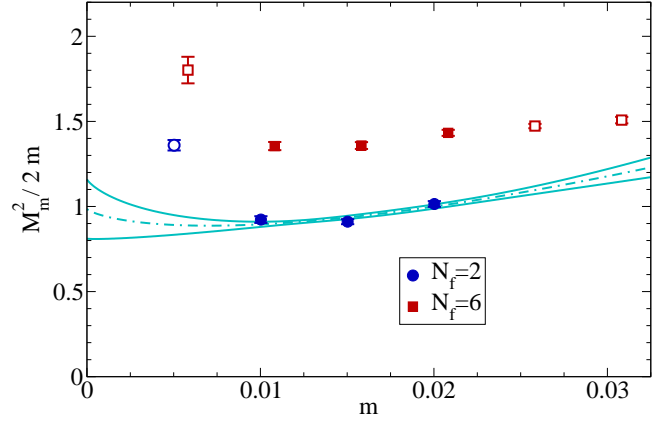
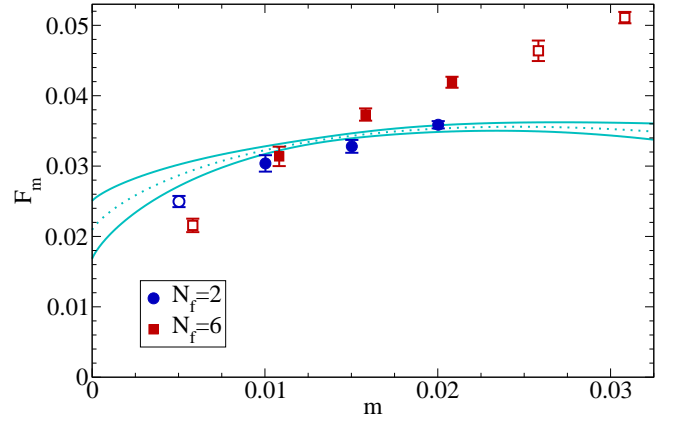
TABLE I: Chirally extrapolated quantities and fit parameters.

FIG. 2: $R_m \equiv [M_m^2/2mF_m]_{6f}/[M_m^2/2mF_m]_{2f}$, versus $\bar{m} \equiv (m(2f)+m(6f))/2$, showing enhancement of $\langle\bar{\psi}\psi\rangle/F^3$ at $N_f = 6$ relative to $N_f = 2$.

we can get an estimate of the enhancement of this ratio by comparing $M_m^2/2mF_m$ at $N_f = 6$ and $N_f = 2$ at finite m_f . We do this by plotting the ratio of ratios $R_m \equiv [M_m^2/2mF_m]_{6f}/[M_m^2/2mF_m]_{2f}$ in Fig. 2. (We use the ratio $M_m^2/2mF_m$ instead of directly evaluating $\langle\bar{\psi}\psi\rangle_m/F_m^3$ because the large contact term in Eq. 3 makes the chiral extrapolation less reliable.) The evident trend is that R_m increases as m_f decreases. Even disregarding the point at $m_f = 0.005$, this suggests that the extrapolated value will be well above unity. A value above 1.5, corresponding to a 50% enhancement of $\langle\bar{\psi}\psi\rangle/F^3$ at $N_f = 6$, will emerge unless there is a downturn in R_m . This would require either a conspiracy of χ PT parameters given the natural upturn of the combined chiral-log terms in Eqs. 1 and 2, or an unexplained and significant downturn before χ PT turns the curve up again as $m \rightarrow 0$.

We nevertheless exercise caution by examining the separate simulation results for $M_m^2/2m$ and F_m , shown in Figs. 3 and 4. While there is good evidence that for $N_f = 2$ a reliable extrapolation of $m \rightarrow 0$ can be performed using NLO χ PT, this is not the case for $N_f = 6$. There, the simulation results for F_m and the linear growth with N_f of the chiral log terms in Eqs. 2 and 3 indicate that the m values are not yet small enough.

We first confirm that for $N_f = 2$, χ PT can be used for the extrapolation. From Figs. 3 and 4, we see that $M_m^2/2m$ and F_m change little in the range $m_f = 0.01 - 0.02$, in-

FIG. 3: The slope of the pseudoscalar mass squared $M_m^2/2m$ in lattice units, as a function of fermion mass. The fit for $N_f = 2$ is from a joint fit to M_m^2 , F_m and $\langle\bar{\psi}\psi\rangle_m$ using the (solid) points at $m_f = 0.01 - 0.02$, constrained to match NLO χ PT.FIG. 4: The Goldstone-boson decay constant F_m in lattice units, as a function of fermion mass. The fit for $N_f = 2$ is a joint fit to M_m^2 , F_m and $\langle\bar{\psi}\psi\rangle_m$, using the (solid) points at $m_f = 0.01 - 0.02$, constrained to match NLO χ PT.

dicating that NLO χ PT (Eqs. 1 and 2) should provide a reliable fit. (Our results for $\langle\bar{\psi}\psi\rangle_m$, not displayed here, show the expected dominance of the linear contact term.) Therefore we carry out the $N_f = 2$ extrapolation $m \rightarrow 0$ using the combined NLO chiral expansions of Eqs. (1), (2) and (3). The five-parameter fit is enumerated in Table I, and the fit curves for $M_m^2/2m$ and F_m , with error bars, are shown in Figs. 3 and 4. Taking covariance into account in error propagation, we find

$$N_f = 2 : \quad \frac{\langle\bar{\psi}\psi\rangle}{F^3} = 47.1(17.6). \quad (4)$$

The values of α_M and α_F indicate the reliability of NLO χ PT, although the χ^2 (Table I) suggests that it may not yet be an excellent fit to the data.

We next compare our $N_f = 2$ results for $\langle\bar{\psi}\psi\rangle/F^3$ and M_ρ/F to the QCD quantities $\langle\bar{q}q\rangle/f_\pi^3$ and m_ρ/f_π ,

a reasonable comparison since the light-quark masses m_q are so small. With $f_\pi = 92.4(0.3)$ MeV and $m_\rho = 775$ MeV, we have $m_\rho/f_\pi = 8.39(0.04)$, compared to our value $M_\rho/F = 9.4(2.5)$. The condensate $\langle\bar{q}q\rangle$ is renormalization-scheme dependent, as is m_q . In the \overline{MS} scheme at 2 GeV ($\simeq 2.6m_\rho$), Ref. [16] finds $\langle\bar{q}q\rangle_{2\text{ GeV}}/f_\pi^3 = 24.1(4.3)$. In our case, $\langle\bar{\psi}\psi\rangle$ is defined by lattice regularization with $a^{-1} \simeq 5M_\rho$ (equivalent to 3.85 GeV). The increase in $\langle\bar{q}q\rangle$ going to this higher scale can be estimated perturbatively from the anomalous dimension of the mass operator [17]. We find $\langle\bar{q}q\rangle_{3.85\text{ GeV}}/f_\pi^3 = 29.5(5.3)$. There is also a renormalization factor $Z^{\overline{MS}}$, which converts the \overline{MS} condensate to the lattice-cutoff scheme. Using Ref. [18], we find $Z^{\overline{MS}}(3.85\text{ GeV}) = 1.227(+37)(-11)$, and therefore $\langle\bar{q}q\rangle_{3.85\text{ GeV,lat}}/f_\pi^3 = 36.2(6.5)$, in agreement with Eq. (4).

Finally, we discuss our $N_f = 6$ results. While the $M_m^2/2m$ values (Fig. 3) change very little in the range $m_f = 0.01 - 0.02$, suggesting that NLO χ PT could be reliable, we have observed that χ PT is unlikely to be reliable for F_m . (The condensate $\langle\bar{\psi}\psi\rangle_m$ (not shown) again varies rapidly, and approximately linearly, indicating the dominance of the contact term.) We argue, though, that a very conservative lower bound can be placed on $\langle\bar{\psi}\psi\rangle/F^3$ by bounding F from above and $\langle\bar{\psi}\psi\rangle/F^2$ from below.

For F_m (Fig. 4), the $N_f = 6$ points at $m_f = 0.01 - 0.02$ decline steeply with decreasing m . The eventual reliability of χ PT (Eq. 2) at lower masses will, because of the negative curvature in the chiral log term, bend the points down even more rapidly. A very conservative *upper* bound on the extrapolated value F should therefore emerge from a linear fit through the three points. This gives $F \leq 0.0208(26)$, essentially the same as the *value* of F in the $N_f = 2$ case. For $M_m^2/2m$ (Fig. 3), the $N_f = 6$ points in the range $m_f = 0.01 - 0.02$ are nearly flat as a function of m . Since χ PT behavior (Eq.1), with its positive curvature, sets in either in this mass range or lower, bending the points up as m is decreased, a very conservative *lower* bound on the extrapolated value $\langle\bar{\psi}\psi\rangle/F^2$ should emerge from a linear fit through these three points. This gives $\langle\bar{\psi}\psi\rangle/F^2 \geq 1.25(5)$.

Together, these give the very conservative lower bound

$$N_f = 6 : \quad \frac{\langle\bar{\psi}\psi\rangle}{F^3} \geq 60.0(8.0). \quad (5)$$

The central value leads to at least a 28% increase relative to $N_f = 2$ (Eq.4), and the absence of enhancement is excluded at the 73% confidence level. We also note that if this quantity is compared to the more precise $N_f = 2$ ratio from QCD phenomenology (36.2 (6.5)), the lower bound on enhancement becomes 30% at 1σ .

Conclusion The ratio $\langle\bar{\psi}\psi\rangle/F^3$ in an $SU(3)$ gauge theory with N_f massless Dirac fermions in the fundamental representation, with the condensate defined by a lattice

cutoff fixed in physical units, is enhanced when N_f is increased from 2 to 6 – by at least 50% from inspection of the simulation results. Even very conservative lower bounds from χ PT-based analyses indicate a substantial increase. An enhancement of less than 50% would require a significant and hard-to-explain downturn in R_m (Fig. 2). We expect the enhancement seen here, arising dominantly at the lattice scale, to be qualitatively the same as with a continuum cutoff from the onset of new physics.

It will be interesting to compare these results with a perturbative \overline{MS} computation of the enhancement based on the anomalous dimension of $\langle\bar{\psi}\psi\rangle$. And it will be important to obtain results for smaller m and perhaps study the chiral extrapolations at NNLO. We must also explore larger values of N_f ($\rightarrow N_f^c$) and other gauge groups, and study the consequences of walking for quark and lepton mass generation and electroweak precision measurements.

We thank LLNL for time on the BlueGene/L supercomputer. This work was supported partially by DOE grants DE-FG02-92ER-40704 (T.A., E.N.), DE-FG02-91ER40676 and DE-FC02-06ER41440, and NSF grants OCI-0749300, DGE-0221680, PHY-0427646 (A.A., R.B., R.C.B., M.A.C., S.D.C., C.R., D.S.), and PHY-0801068 (G.F.). It was also supported by the DOE through ANL under contract DE-AC02-06CH11357 (J.O.), and the DOE Office of High Energy Physics through LLNL under contract DE-AC52-07NA27344 (M.C., R.S., P.V.).

-
- [1] W. E. Caswell, Phys. Rev. Lett. **33**, 244 (1974).
 - [2] T. Appelquist, G. T. Fleming, and E. T. Neil, Phys. Rev. Lett. **100**, 171607 (2008), 0712.0609.
 - [3] A. Deuzeman, M. P. Lombardo, and E. Pallante, Phys. Lett. **B670**, 41 (2008), 0804.2905.
 - [4] T. Appelquist, G. T. Fleming, and E. T. Neil, Phys. Rev. **D79**, 076010 (2009), 0901.3766.
 - [5] A. Deuzeman, M. P. Lombardo, and E. Pallante (2009), 0904.4662.
 - [6] Z. Fodor, K. Holland, J. Kuti, D. Negradi, and C. Schroeder (2009), 0907.4562.
 - [7] K. Yamawaki, M. Bando, and K.-i. Matumoto, Phys. Rev. Lett. **56**, 1335 (1986).
 - [8] T. W. Appelquist, D. Karabali, and L. C. R. Wijewardhana, Phys. Rev. Lett. **57**, 957 (1986).
 - [9] R. Sommer, Nucl. Phys. **B411**, 839 (1994).
 - [10] J. Gasser and H. Leutwyler, Phys. Lett. **B184**, 83 (1987).
 - [11] D. B. Leinweber, A. W. Thomas, K. Tsushima, and S. V. Wright, Phys. Rev. **D64**, 094502 (2001), hep-lat/0104013.
 - [12] C. Allton et al. (RBC-UKQCD), Phys. Rev. **D78**, 114509 (2008), 0804.0473.
 - [13] H. Leutwyler and A. V. Smilga, Phys. Rev. **D46**, 5607 (1992).
 - [14] C. Jung, PoS **LAT2009**, 002 (2009).
 - [15] A. Gray et al., Phys. Rev. **D72**, 094507 (2005).
 - [16] M. Jamin, Phys. Lett. **B538**, 71 (2002), hep-ph/0201174.
 - [17] J. A. M. Vermaseren, S. A. Larin, and T. van Ritbergen,

Phys. Lett. **B405**, 327 (1997), hep-ph/9703284.

[18] S. Aoki, T. Izubuchi, Y. Kuramashi, and Y. Taniguchi, Phys.

Rev. **D67**, 094502 (2003), hep-lat/0206013.